RAY W. HERRICK LABORATORIES

A Graduate Research Facility
of The School of Mechanical Engineering

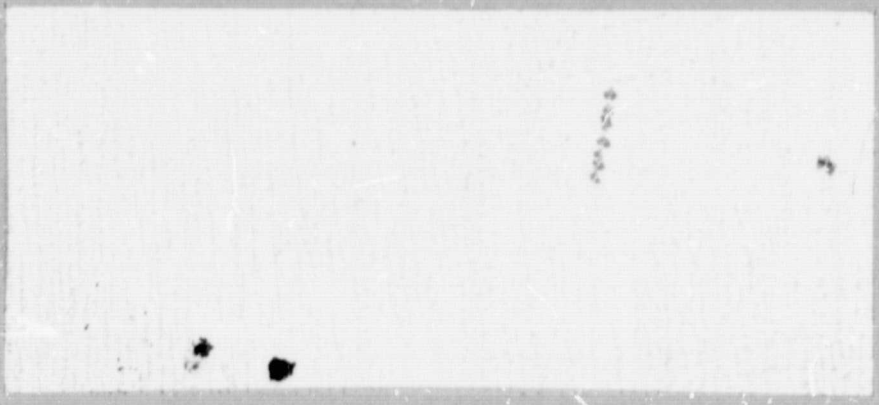

Purdue University

West Lafayette, Indiana 47907

A STUDY OF METHODS TO PREDICT AND MEASURE THE TRANSMISSION OF SOUND THROUGH THE WALLS OF LIGHT AIRCRAFT

Research Contract #0226-52-1288

PREDICTION OF LIGHT AIRCRAFT INTERIOR SOUND PRESSURE LEVEL USING THE ROOM EQUATION

Sponsored by

NASA
Hampton, VA 22365

Report No. # 0226-12 HL 84-15

Submitted by:

Mahabir Atwal, Visiting Scholar
Robert Bernhard, Principal Investigator

Approved by:

Raymond Cohen, Director
Ray W. Herrick Laboratories

May 1984

1. INTRODUCTION

During recent years, there has been growing interest in reducing the interior noise levels of propeller driven aircraft. This is not only because the noise levels in many such aircrafts exceed acceptable comfort limits, but also because of the large demand for propeller driven passenger aircrafts which are nearly 20% more fuel efficient than jet aircrafts having otherwise comparable technology. The major noise components in such aircrafts are below 100 Hz and the interior noise spectra generally consists of low frequency broadband characteristics with discrete frequency peaks which can be identified as harmonics of both the blade passage and engine firing frequency.

For interior aircraft noise reduction studies, in addition to determining the major sound transmission paths, one must also be able to examine the effect on the interior noise of changing certain cabin parameters, such as increasing the cabin wall transmission loss or increasing the interior absorption. It would be most useful to small aircraft manufacturers, if the feasibility of such changes could be examined by using a simple theoretical model prior to making the changes. Interior noise prediction methods in common use in the aircraft industry generally look at the modes of the structure and the interior space in order to predict the interior noise. Such schemes can be very complex and the determination of the various properties of the structure can be difficult experimentally. Such schemes often reproduce experimental trends but predicted levels may differ by

10 dB or more from measured values in certain frequency bands (1). In the present study the feasibility of using the room equation (2), which is based on power balance, and uses the measured acoustic intensity data, has been investigated as a scheme to predict the interior sound pressure level. The emphasis in this study was on a simple model requiring uncomplicated experimental techniques, which it was felt may be more useful to small aircraft manufacturers, who may not have the resources or the facilities to use a complicated model. The validity of this model in predicting the interior cabin sound pressure level for different fuselage and exterior sound field conditions is presented. The fuselage of a small single engine Piper Cherokee aircraft (Model PA 28-140) shown in Fig. 1 was the subject of the tests presented in this study.

1.1 Prediction of Interior Sound Pressure Level Model

The basic approach followed in predicting the interior cabin sound pressure level is that of making an acoustic power balance. This is achieved by equating the net power flow into the cabin volume to the power dissipated within the cabin volume using the room equation.

$$L_p = L_W + 10 \log \left(\frac{Q}{4\bar{\Lambda} r^2} + \frac{4}{R}\right) \qquad (1)$$

where L_p is the sound pressure level at the measurement point, L_W is the sound power level emitted by the source, Q is the directivity factor, r is the distance from the source to the measure-

ment point and R is the interior room constant. The room constant is defined as

$$R = \frac{S_o \bar{\alpha}}{(1-\bar{\alpha})} \tag{2}$$

where $\bar{\alpha}$ is the average absorption coefficient of the interior surface of the cabin and S_o is the total interior surface area of the cabin. The average adsorption coefficient can be expressed in terms of the reverberation time of the cabin (T_R), using the equation

$$T_R = \frac{0.161V}{-S_o \ln (1-\bar{\alpha})} \tag{3}$$

where V is the volume of the enclosure. Thus

$$R = S \left(1 + e^{\frac{.161V}{T_R S}}\right) \tag{4}$$

The room constant of the cabin was calculated from the measured reverberation time using Eq. (4). Initial studies showed that for the order of magnitude of the reverberation time of the cabin, the room equation was very sensitive to small changes in the reverberation time. As such great care was taken to measure the reverbation time accurately. The reverberation time of the cabin was measured using a specially written Fortran program on the FFT, as conventional level recorder method proved to be inaccurate because of the very short decay rate. The reverberation time measurement procedure is discussed in detail in the appendix.

1.2 Cabin Interior Noise Prediction in an Reverberant Field

Validation of the room equation to predict the interior sound pressure level of the cabin in a reverberant field was performed with the fuselage suspended in the reverberation chamber. All tests were carried out on 8 panels shown in Fig. 2 with at least two sheets of lead-vinyl on all other exterior parts of the fuselage. In the analysis it was assumed that sound energy enters the cabin only through the eight panels with no leakage through other parts of the fuselage. The interior end exterior sound pressure levels were measured using the experimental set up shown in Fig. 3. The sound power level transmitted through the panels in Eq. 1, was calculated by multiplying the measured space averaged transmitted intensity for each individual panel by its surface area. The level of transmitted intensity (L_{It}) for a particular panel was calculated using the expression

$$L_{It} = L_{Ii} - T.L. = L_{Pe} - 6 - T.L.$$

where L_{Ii} is the level of incident intensity, T.L. is the panel transmission loss and L_{Pe} is the exterior sound pressure level. The transmission loss of the panels was measured using the two-microphone acoustic intensity technique (3).

By assuming the directivity factor to be unity, the sound pressure level L_{P_i}, at a chosen location in the cabin was calculated for one panel. Assuming the acoustic pressures transmitted through the panels are incoherent, the overall sound pressure level was obtained by summing the mean square sound pressures

radiated from each of the eight panels under consideration. The overall sound pressure level calculations were performed at several locations within the cabin. The locations were chosen to represent points every 3 degree on a circle, representing the rotation of the microphone used to measure the interior sound pressure level as shown in Fig. 4. From these calculations an average value was calculated, to represent the space averaged interior cabin sound pressure level. This level was than compared with the measured values. The comparison was made for two different fuselage conditions: first, all eight panels under study in the as-manufactured state and second, all windows covered with one sheet of lead-vinyl but aluminum panels in the as-manufactured state. Figures 5 and 6 show the respective comparison between the predicted and measured space averaged sound pressure level.

Keeping in mind that the room equation model used to predict the interior sound pressure level is a very simple model, requiring simple experimental measurements. However, as seen in Fig. 5, for the as manufactured state, the predicted and measured results agree fairly well. In the second case Fig. 6, the agreement below 500 Hz is also very good, the main frequency region of interest for such aircrafts. The discrepancy at high frequencies may be due to the fact that only eight areas were considered to be radiating sound power into the cabin in the prediction scheme. However, there may be other areas which become important at high frequencies specially when the windows are covered. If there are

such areas or leaks, than the measured interior sound pressure level as indicated will be higher than the predicted. In the first case Fig. 5, the windows are the dominant paths of sound transmission and the effect of leaks in comparison with the second case Fig. 6, will be small. Because when the windows are covered, the leaks will become important at high frequencies, where the transmission loss of the lead covering is high.

1.3 Cabin Interior Noise Prediction in a Semi-Anechoic Environment

In order to distinguish whether the discrepancies in the last section between the predicted and the measured cabin interior sound pressure level were the cause of leaks or inconsistency of measured and predicted results. The fuselage was moved to the semi-anechoic chamber, where it was subjected to a direct sound field from one source. With this experimental arrangement, it was felt, the leaks or flanking paths if responsible for the discrepancies will become less important, because the field can be more localized on the areas under study.

As before, the sound power level transmitted through the panels in Eq. 1, was calculated by multiplying the measured space averaged transmitted intensities for each individual panel by its surface area. The experimental set-up for the measurement of the transmitted intensities and sound pressure is shown in Fig. 7. In this part of the study all tests were performed by changing the back two panels (1 and 2, Fig. 2) only and with at least two

sheets of lead-vinyl on all other parts of the fuselage. The increased attenuation due to lead-vinyl in conjunction with decreased incident sound power on other panels made it possible to assume that the sound radiating into the cabin by these paths was negligible compared to panels 1 and 2. However, because the door plexiglass window and aluminum panel were located close to the back panels under consideration, it was felt that sound power radiated by the door panels should also be taken into consideration in the prediction scheme, even though they were covered with lead-vinyl all the time.

Transmitted intensity and interior sound pressure level data was collected for three different back panel conditions namely both panels in the as-manufactured conditions, both panels covered with one sheet of lead-vinyl and finally plexiglass window covered with one sheet of lead-vinyl but with the aluminum panel in the as-manufactured condition. For each condition the intensity transmitted by the door panels (3 and 4, Fig. 2) lead-vinyl combination was also measured. Using measured values of reverberation time and transmitted intensities, the room equation was used to predict the space averaged interior sound pressure level for the three different conditions. The power radiated into the cabin interior was a sum of the power radiated by the four areas and was calculated for each individual panel by multiplying the measured space averaged transmitted intensity by its surface area. Figures 8, 9 and 10 show the comparison between the measured and predicted space averaged sound pressure levels for

the three panel conditions. A fairly good agreement, for all three conditions, is observed throughout the frequency range.

2. CONCLUSION

The validity of the room equation model to predict the cabin interior sound pressure level was supported by experimental data for different fuselage and incident sound field conditions. The room equation is obviously a highly simplified model of the real problem requiring simple experimental measurements. However, the general agreement between the room equation and experimental test data was considered good enough to be used for preliminary design studies.

3. REFERENCES

1. Wilby, J.F., "The Prediction of Interior Noise of Propeller Driven Aircraft: A Review," SAE Technical Paper 830737, April 1982.

2. Irwin, J.D. and Garf, E.R., "Industrial Noise and Vibration Control," Prentice-Hall, Inc., Chapter 6 (1979).

3. Atwal, M., David, J., Heitman, K., Crocker, M., "Light Aircraft Sound Transmission Study," Herrick Laboratories Report, HL 83-21, August (1983), Mechanical Engineering, Purdue University, West Lafayette, In 47907.

APPENDIX

4. MEASUREMENT OF REVERBERATION TIME

The reverberation time is the time required for the acoustic energy density in an enclosure to decay 60 dB. Figure 11 shows the instrumentation used to measure the reverberation time. The signal to the loudspeaker (an 8" 15W Calrad) was filtered so that the speaker emitted only frequencies in a specific one-third octane band. The cone of the loudspeaker was laid on top of the dashboard facing the windshield to make the acoustic power output to the cabin as large as possible. The seats were retained in the fuselage to make the cabin interior more realistic. A half-inch, field-incidence microphone on a boom rotating at a radius of about 0.3 was positioned near the center of the cabin, as shown in Fig. 4. The boom was rotated at a rate of one revolution every 64 seconds, at this rate smearing of the data due to change in microphone position was minimized.

The measurement system operates using the interrupted noise method. The relay starts and stops the sound source and operates the recording of sound decay spectra on the FFT as soon as the sound source is turned off. The recorded decay spectrum is then stored in the memory of the FFT, and a new decay spectrum is taken, allowing enough time for the sound field in the cabin to reach steady state conditions. The new spectrum is added to the first and the sum is stored in the memory of the FFT. In case of

relay malfunction, option is available to reject any spectrum if required. The process is repeated several times depending on the accuracy required and each time the new decay spectrum is added to the sum of the previous decay spectra. The reverberation time is then determined from the initial slope of the mean decay spectra. In this study, fifty samples were averaged for each one-third octane band measurements. For all but the lowest one-third octane bands (100 and 125 Hz), the mean decay spectra was a distinct straight line. Figure 12 shows the variation of the cabin reverberation time with frequency measured using this approach.

Figure 1. Photograph of Piper Cherokee fuselage in the reverberation chamber.

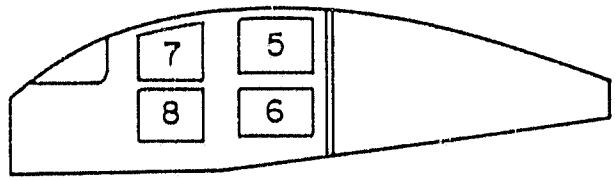

Left Side

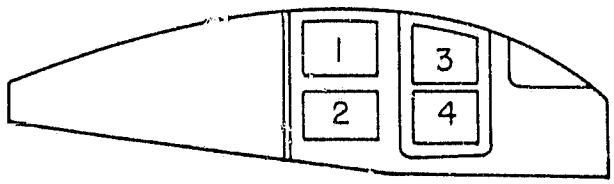

Right Side

1,3,5,7 - Plexiglas Windows
2,4,6,8 - Panels

Figure 2. Panels of fuselage studied in the experiments.

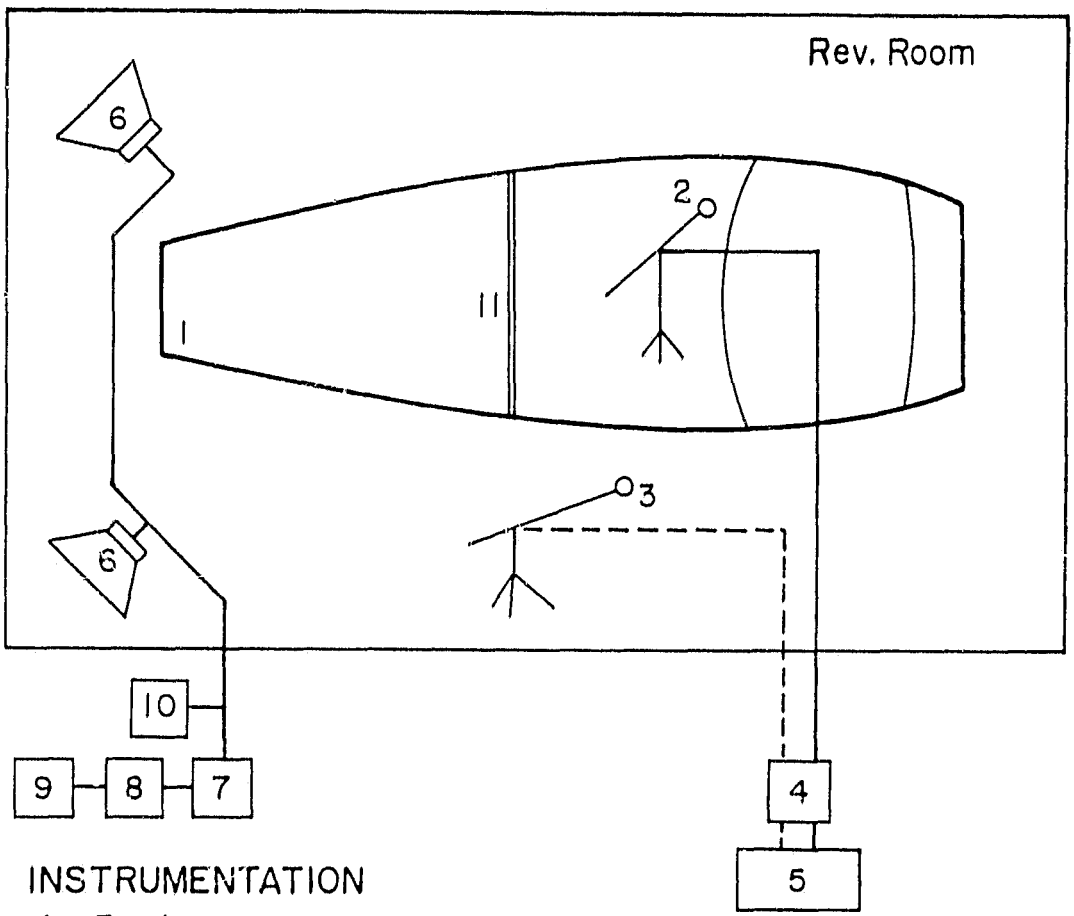

INSTRUMENTATION

1. Fuselage
2. Rotating Microphone Boom
3. Rotating Microphone Boom
4. Microphone Amplifier
5. Fast Fourier Transform Analyzer (FFT)
6. Speaker
7. Filter
8. Amplifier
9. Random Noise Generator
10. Random Noise Voltmeter
11. Plywood-Fiberglass Divider

Figure 3. Experimental set-up for the measurement of interior and exterior sound pressure level (fuselage in reverberation chamber).

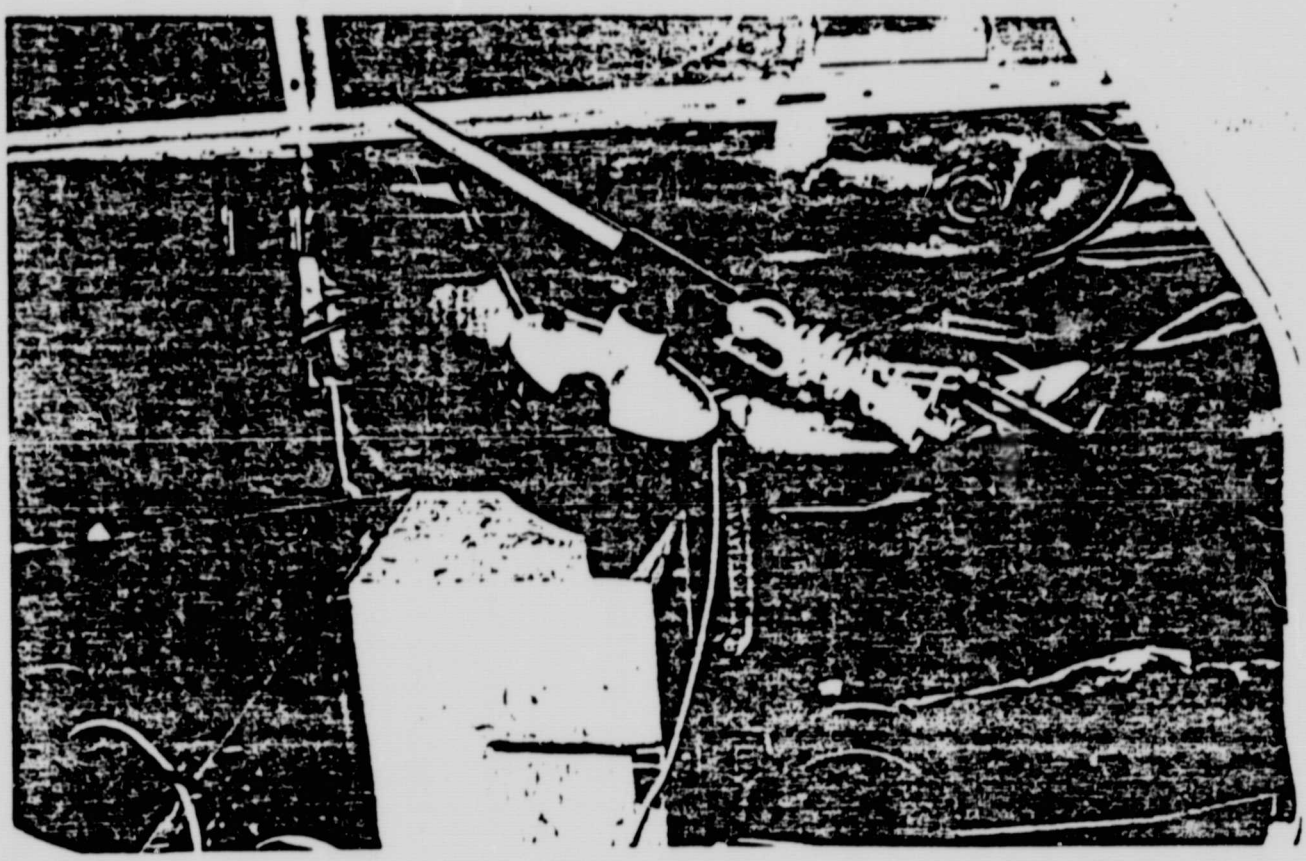

Figure 4 Photograph of microphore apparatus used to measure the space-averaged interior sound pressure level.

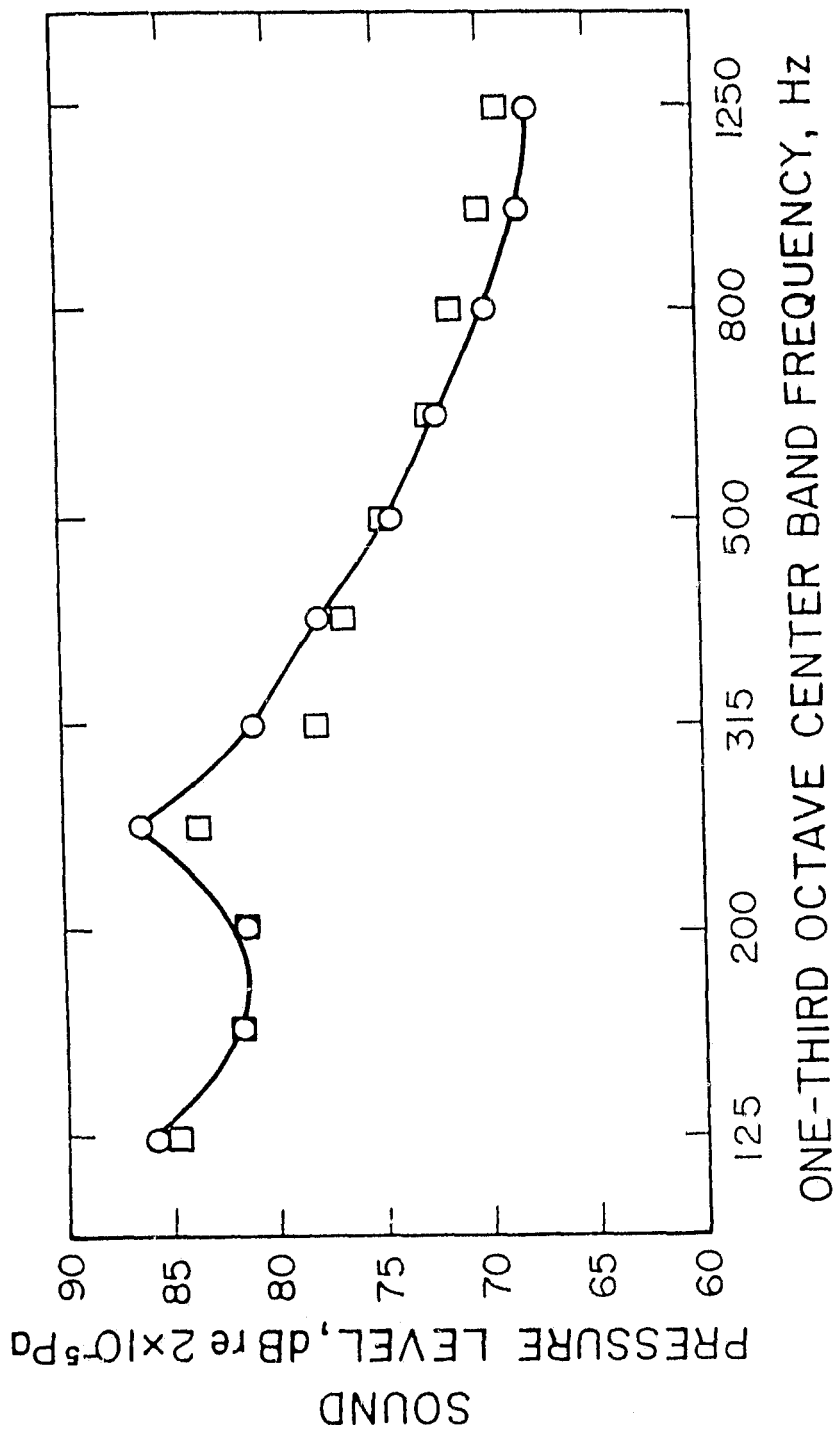

Figure 5. Interior sound pressure level for the panels in the as-manufactured condition in a reverberation field ⊡ measured -x-x predicted.

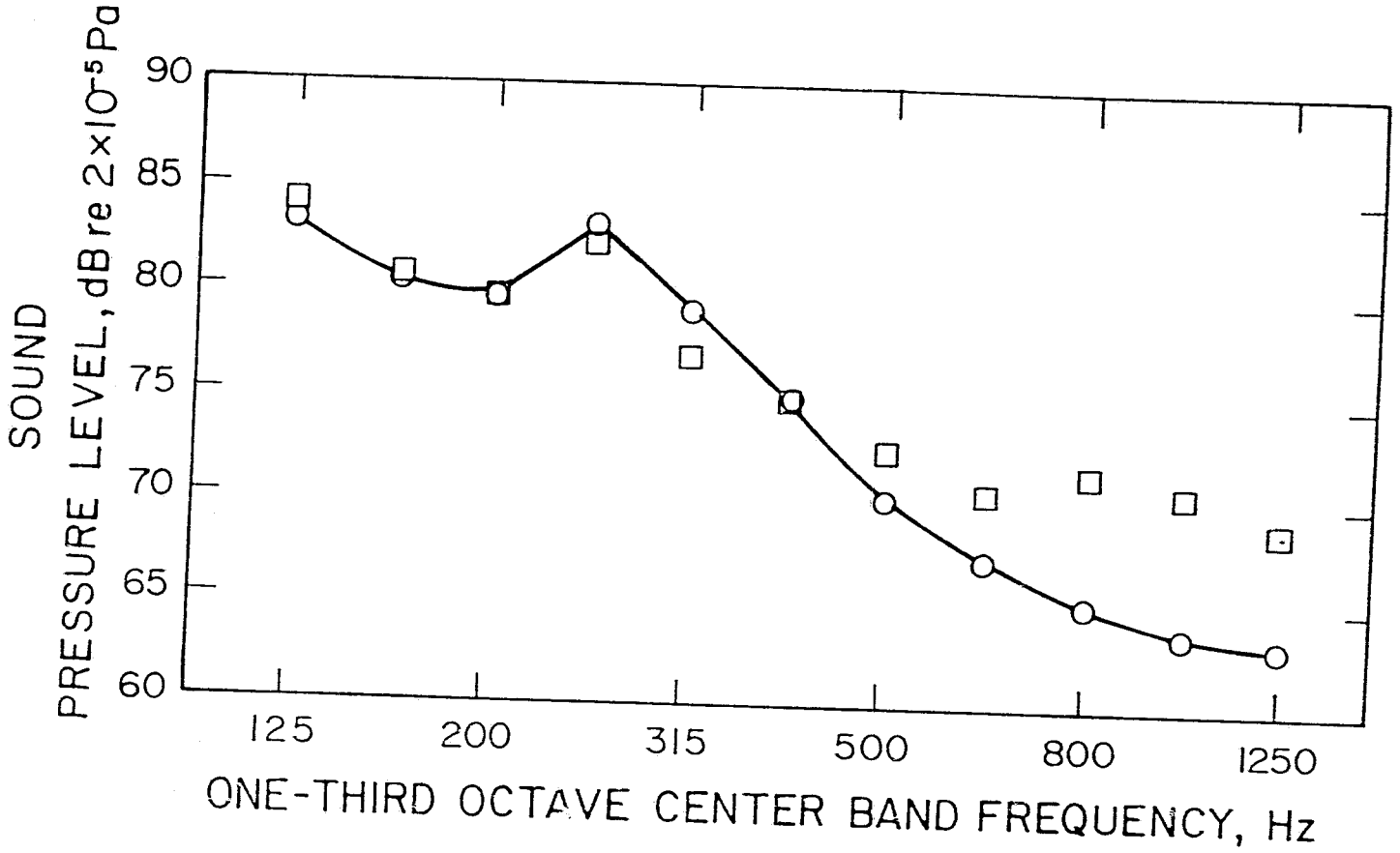

Figure 6. Interior sound pressure level for the windows covered in a reverberant field ⊡ measured x-x- predicted.

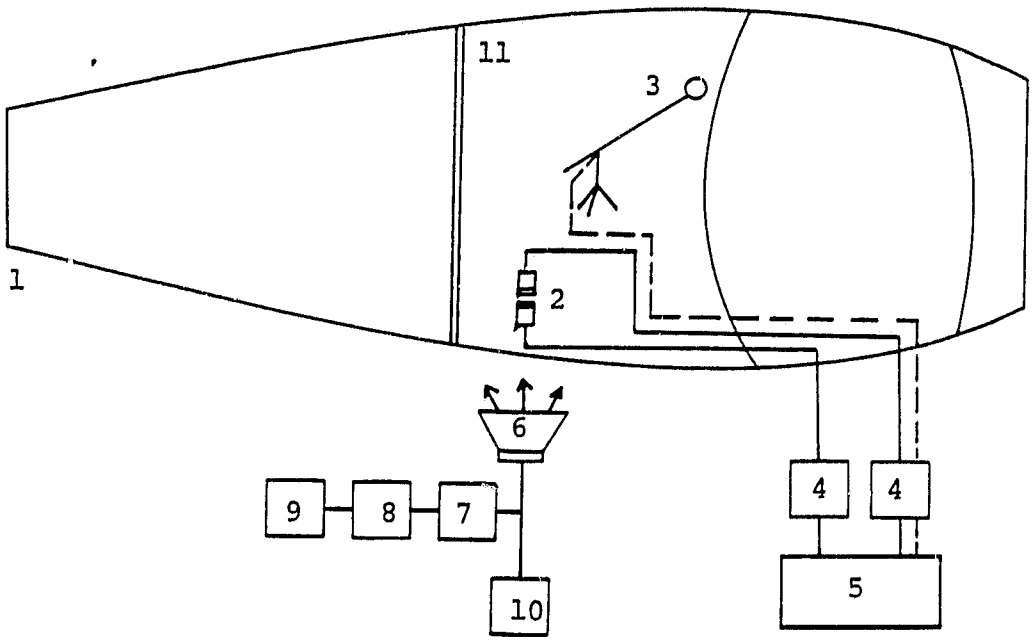

INSTRUMENTATION

1. Fuselage
2. Phase-Matched Microphones
3. Interior Rotating Microphone
4. Measuring Amplifier
5. Fast Fourier Transform Analyzer (FFT)
6. Speaker
7. Filter
8. Amplifier
9. Random Noise Generator
10. Random Noise Voltmeter
11. Plywood-Fiberglass Divider

Figure 7. Experimental set-up for measurement of transmitted intensities and sound pressure levels in semi-anechoic chamber.

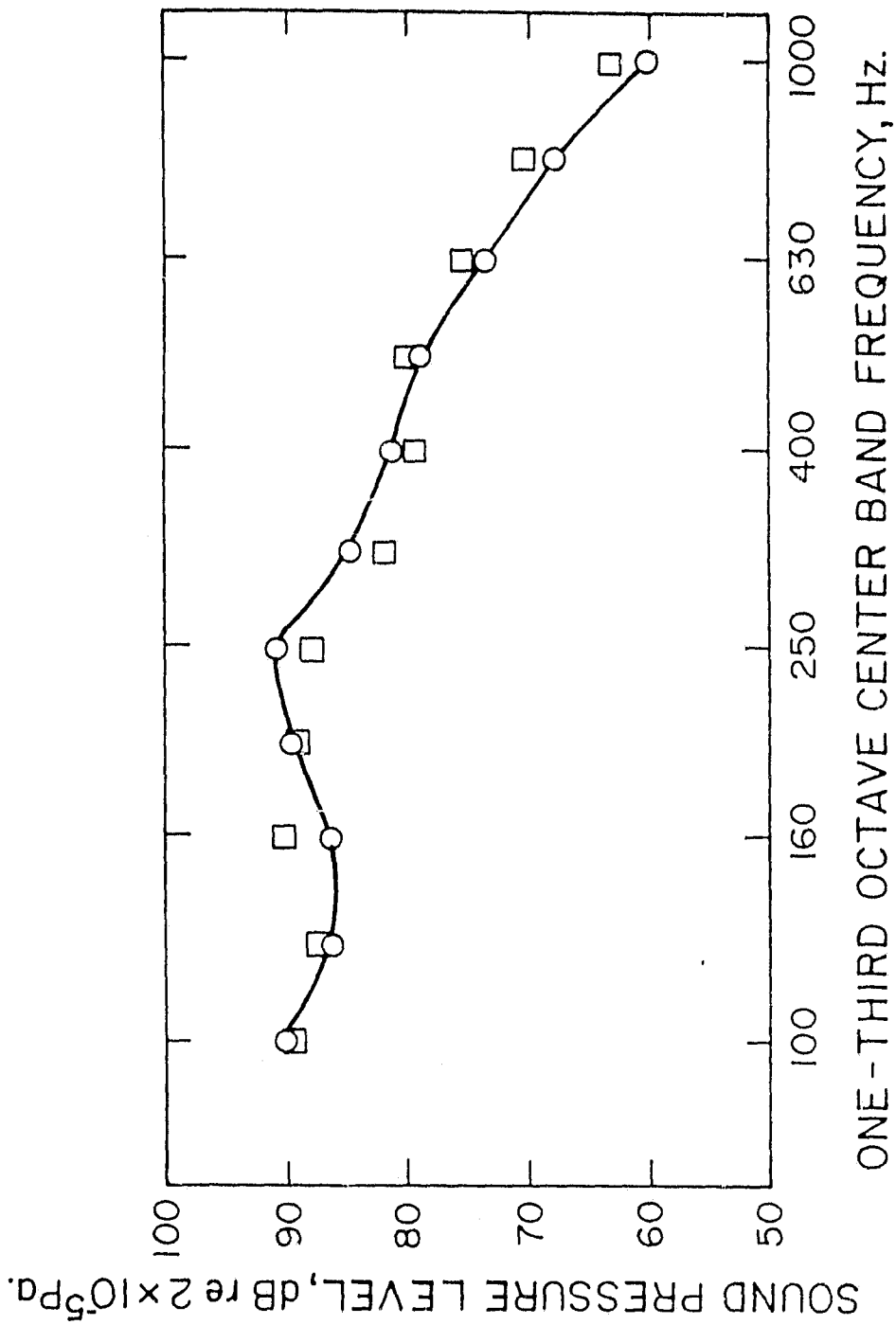

Figure 8. Interior sound pressure level for the panels in the as-manufactured condition in a direct field.
⊡⊡ measured -x-x predicted

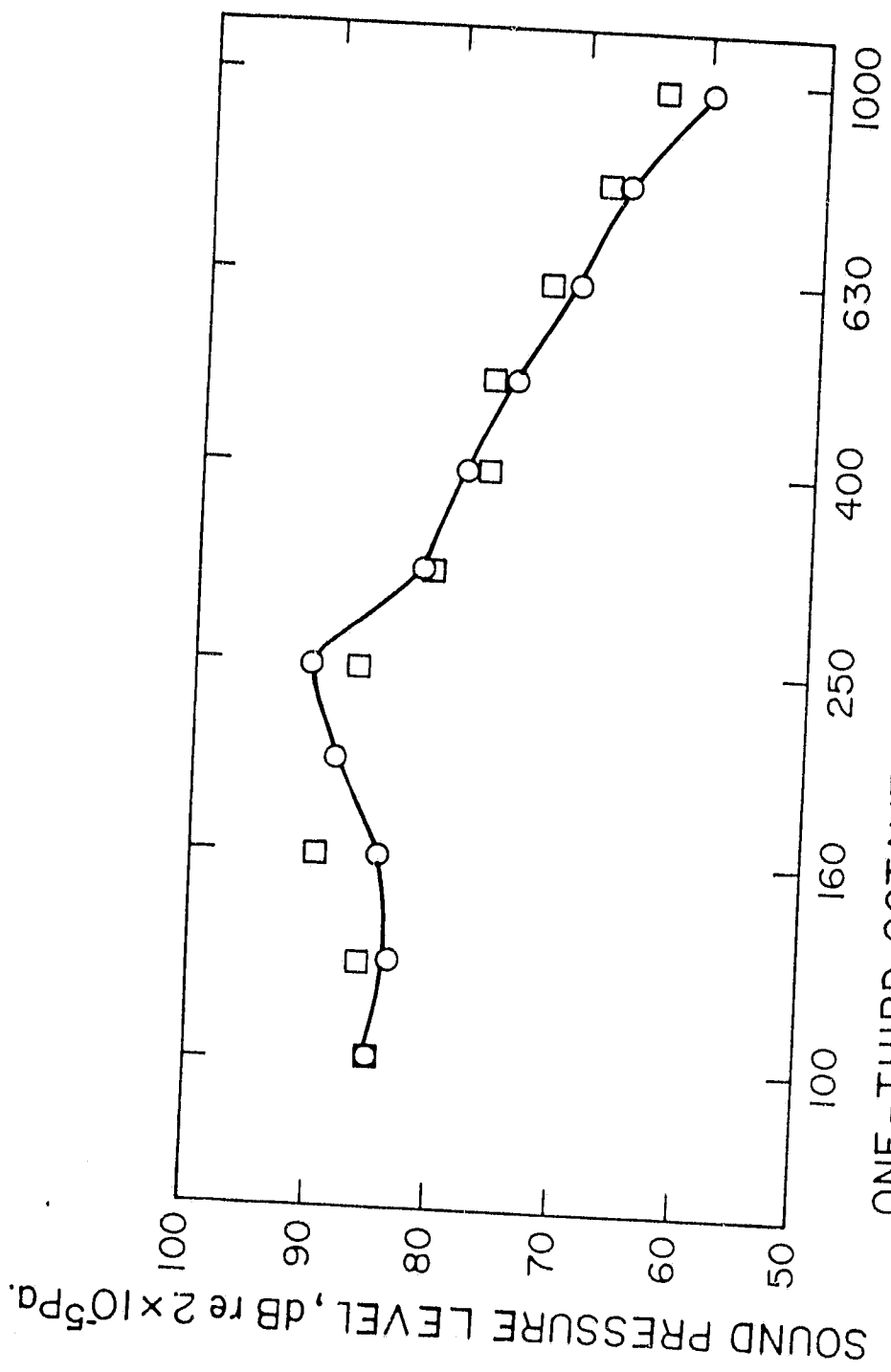

Figure 9. Interior sound pressure level for the window only covered with one sheet of leaded-vinyl in a direct field.
□□ measured, -x-x- predicted.

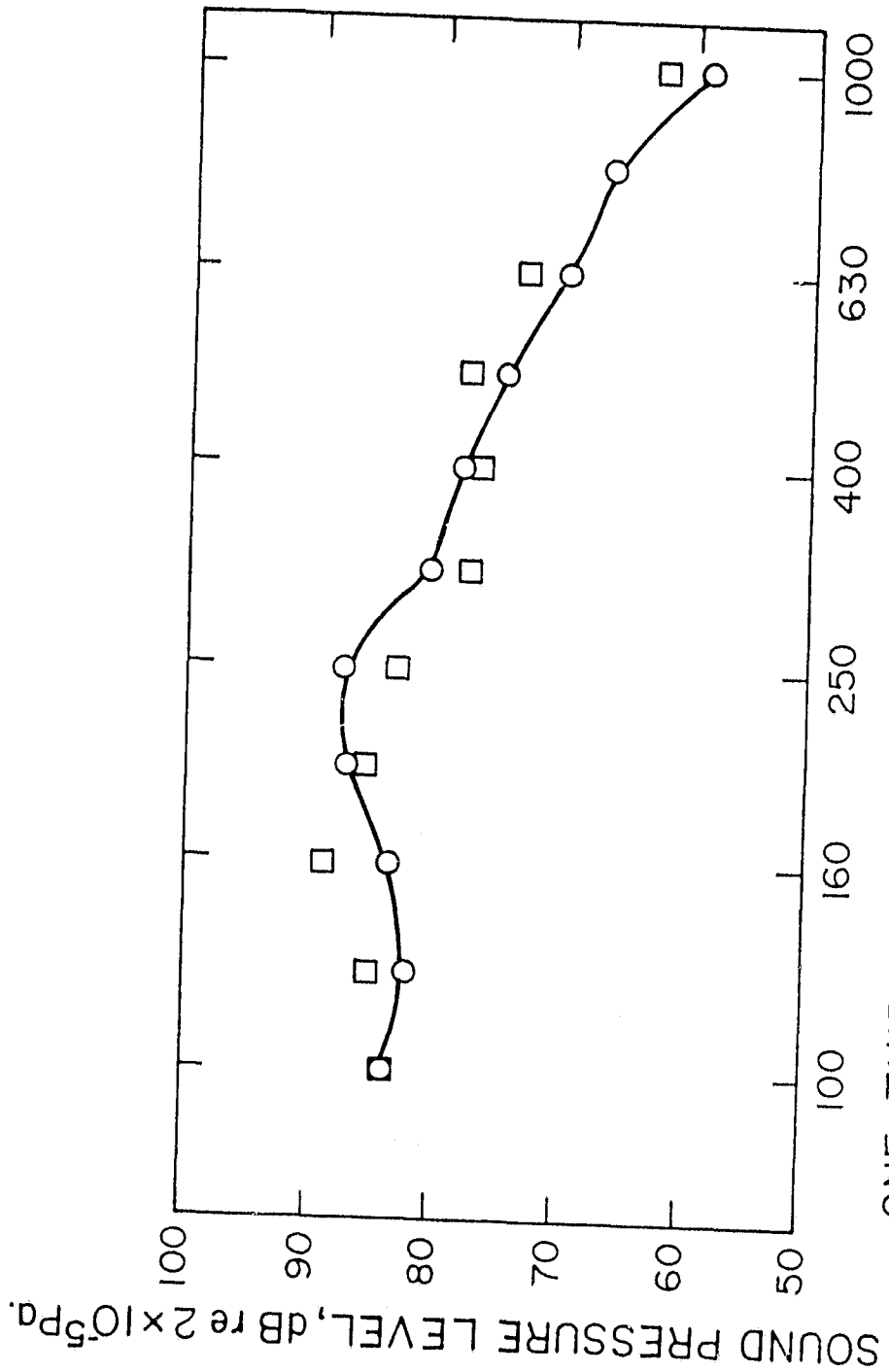

Figure 10. Interior sound pressure level for the window and panel covered with one sheet of lead-vinyl in a direct field. ⊡⊡ measured, -x-x- predicted.

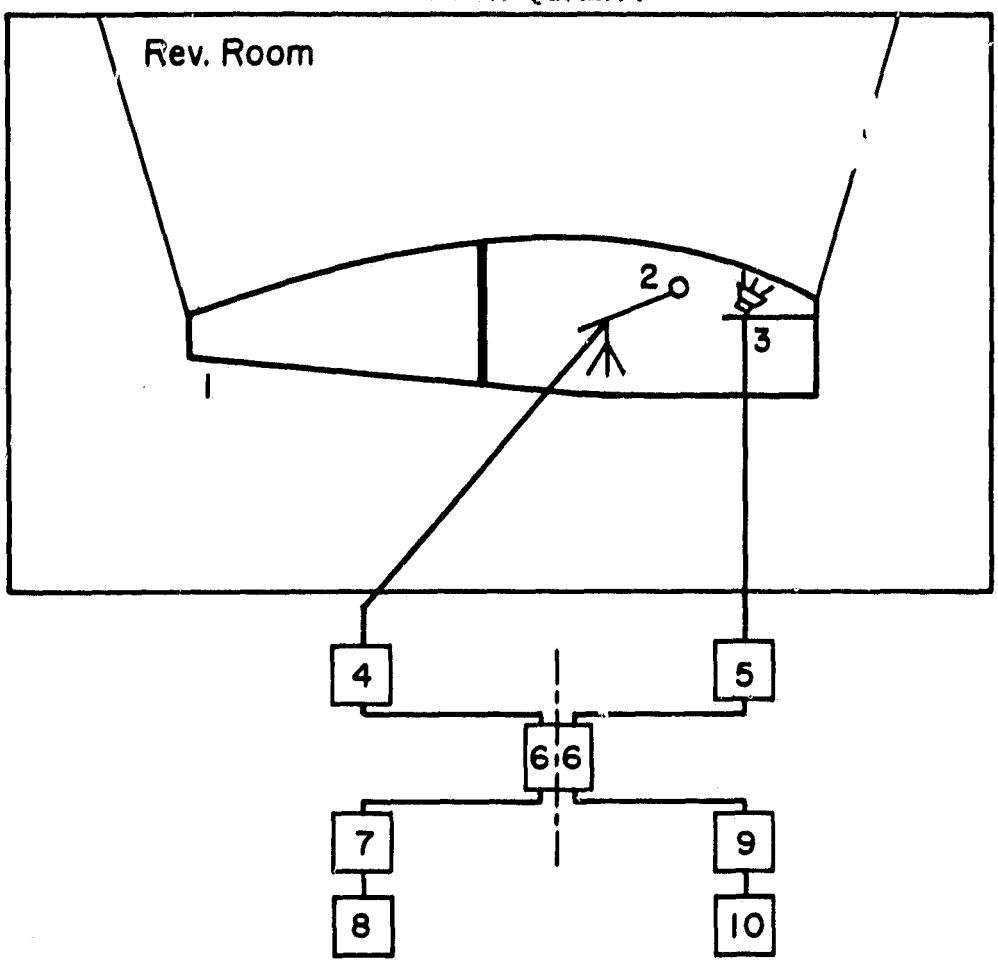

INSTRUMENTATION

1. Fuselage
2. Rotating Microphone Boom
3. Loudspeaker
4. Microphone Amplifier
5. Amplifier
6. Relay
7. Anti-Aliasing Filter
8. Fast Fourier Transform Analyzer (FFT)
9. One-Third Octave Band Filter
10. Beat Frequency Oscillator

Figure 11. Experimental set-up for measurement of reverberation time.

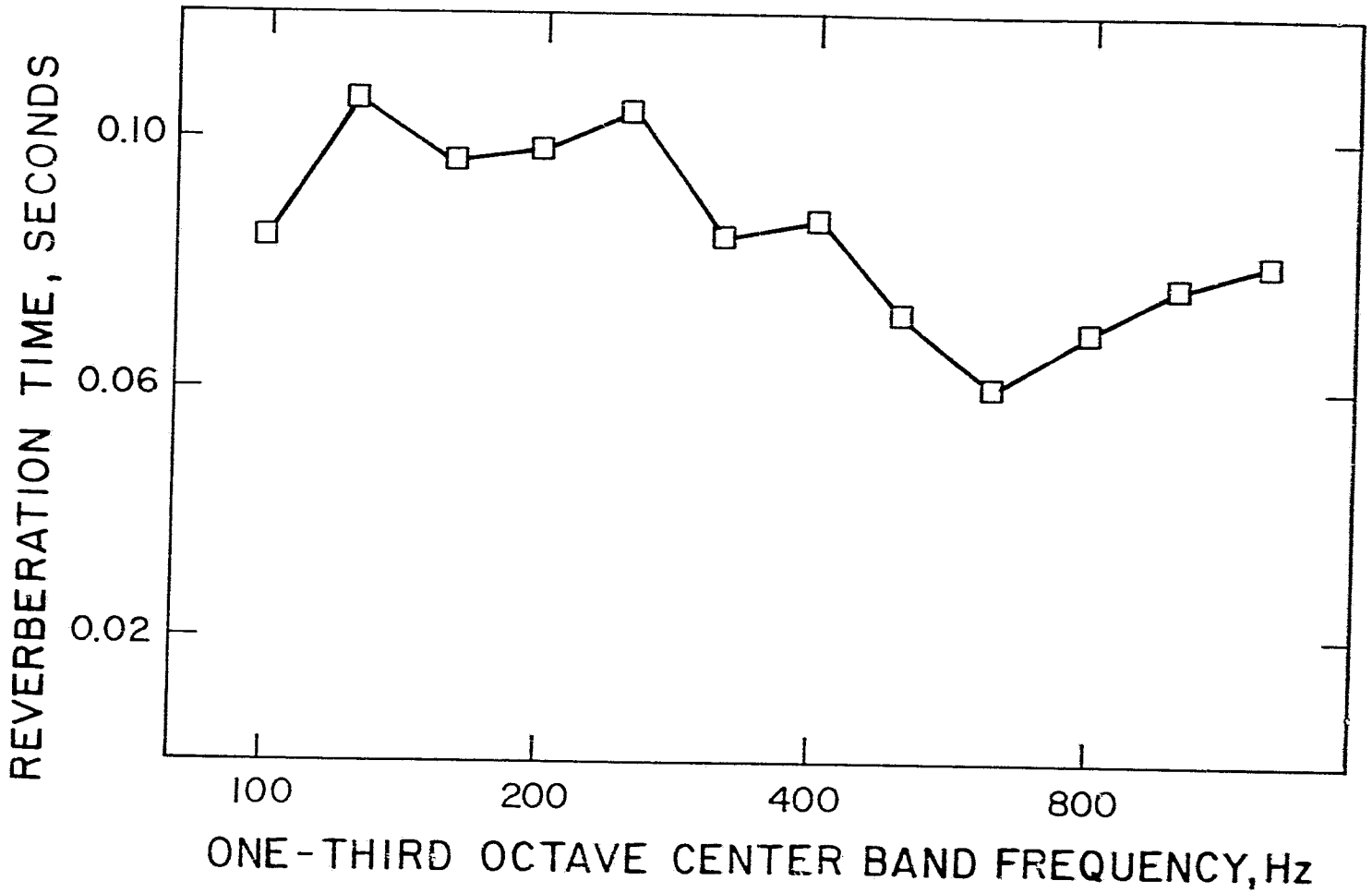

Figure 12. Reverberation time vs. frequency for the cabin.